

Hydrogen temperature gradient in the transition region of a solar coronal hole

E. Marsch¹, C.-Y. Tu^{1,2}, and K. Wilhelm¹

¹ Max-Planck-Institut für Aeronomie, 37191 Katlenburg-Lindau, Germany

² Department of Geophysics, Peking University, Beijing, 100871, P.R. China

Received 10 February 2000 / Accepted 14 April 2000

Abstract. The Lyman series of hydrogen was observed by SUMER on SOHO on the north polar limb of the Sun with a total exposure time of more than ten hours. The resulting line profiles have been analysed using the technique described by Marsch et al. (1999). The data analysis corroborates earlier findings on the Lyman lines, but also yields phenomena which cannot be fully understood at the present time. Firstly, the line width of the Lyman lines increases with decreasing series or quantum number. Secondly, the hydrogen temperature gradient in the height range from 12 000 km to 18 000 km is unexpectedly small and does not reveal a steep jump as might be expected from modelling of the transition region. The average temperature increases only slightly from $1 \cdot 10^5$ K to $2 \cdot 10^5$ K. Possible explanations of these observations are given and models are briefly discussed.

Key words: line: profiles – Sun: corona – Sun: UV radiation

1. Introduction

In a recent paper, Marsch et al. (1999) suggested a new method to measure the hydrogen (and proton) temperature on and off the solar limb by using the hydrogen Lyman lines, of which more than 20 can be clearly resolved by SUMER on SOHO (Wilhelm et al., 1997a; Warren et al., 1998; Curdt and Heinzel, 1998). The line shapes and intensities were obtained versus height ranging from about $10''$ to $70''$ above the photospheric limb. The lines are relatively broad and show the typical self-absorption reversal near the limb, where the emission comes from optically thick material, and then change systematically in shape with increasing height. The H I Ly5, Ly6, Ly7, Ly9, Ly10 and Ly11 lines attain a Gaussian shape at different locations within a small height range, i.e., between about $12''$ and $23''$ ($1'' \approx 715$ km), a range which is determined by the fact that opacity effects terminate the analysis at lower heights and scattered light contributions at greater heights. The line width is explained as being caused by Doppler broadening transforming into an effective temperature of the hydrogen gas, in which wave-turbulence and ion-kinetic or thermal components are usually included. This explanation is supported by a radiative transfer model calculation, which

was used already and discussed in Marsch et al. (1999). At even greater heights, the line intensities are rather low, and the profiles show again the typical self-absorption features. These lines stem from radiation originally emitted from the disk and represent light scattered by the finite surface roughness of the SUMER telescope mirror. The level of straylight was estimated by Marsch et al. (1999) and found to be such that the Gaussian profiles are not significantly affected near $15''$.

The temperature gradient in the lower solar atmosphere is very important, since it determines the conduction of heat and is intimately related with the overall energy balance of the transition region (TR). Classical single-fluid TR models (see., e.g., Vernazza et al., 1973; Vernazza et al., 1981; Chae et al., 1998; or the Chapters 6 and 7 in the book of Mariska, 1992), while assuming a large electron heat conductivity, result in a very steep temperature gradient with height (with an intrinsic scale of about only 100 km). However, there have not yet been reported any reliable observations of the proton or hydrogen temperature profiles at these heights. Some observations show that the height profiles of emission line radiances (Wilhelm et al., 1998a) from heavy ions with high and low ionization states (for example, N V and S II, Marsch et al., 1997, or Feldman et al., 1976, who also studied these lines from Skylab data) have their maximum at about $10''$, perhaps indicating an inhomogeneous distribution of plasma at widely different temperatures, which is also frequently observed (Fludra et al., 1997) higher up in the corona in hotter emission lines seen with the Coronal Diagnostic Spectrometer (CDS) on SOHO. However, direct information about the proton temperature is direly needed. This cannot be obtained by any direct spectroscopic means, since the protons, trivially to say, do not radiate and are thus elusive of remote sensing. Therefore, we use here again the technique employed by Marsch et al. (1999) to analyse a new SUMER data set. This was obtained with a longer exposure time than previously, with the intention to establish the hydrogen and (given that the strong charge-exchange-induced coupling equilibrates their temperatures) proton temperature gradient in the solar TR.

2. Data analysis and results

To analyse the proton and hydrogen temperatures at the base of the solar polar corona we exploit the hydrogen temperature gra-

Table 1. Description of data sets

Data set	Observation	Slit size	Centre of slit (Sun x, Sun y)	Exposure time × number of images	Spectral range pixels; Å
1	7 March 1999	1'' × 120''	(0'', 995.25'')	110 s × 346	1024; 46
2	7 November 1998	1'' × 120''	(0'', 1020'')	115 s × 161	1024; 46

dient as obtained from near-limb observations of the H I Lyman series in the polar regions of the Sun. The description of the data is given in Table 1. We essentially use the data set 1, which was obtained from a limb observation in the middle of the northern polar coronal hole. The spectral range covers the Lyman series from Ly5 to Ly11. The long total exposure time (more than 10 hours) ensures good photon statistics and allows us to use small height bins of only 2'' in size. With this we can resolve the radial gradient of the line profiles as good as possible and make almost full use of SUMER's spatial resolution capability. At each height bin we have calculated the averaged line profile for each of the six Lyman lines selected. For each Lyman line we identified a narrow height range in which a Gaussian-type line profile was obtained. At lower heights opacity effects determine the line shape, while higher up the light scattered from the telescope mirror determines the line shapes, essentially being copies of the shapes of the lines as emitted directly at the limb below 3 000 km or from the disk. Since Gaussian profiles appear in a narrow height range from 12'' to 23'', we can study their widths and the inferred temperature variation only in this small height range.

The SUMER instrument, its in-flight performance and first results are described in Wilhelm et al. (1995, 1997a) and Lemaire et al. (1997). The data preparation for this analysis follows the standard SUMER procedures (see, e.g., Curdt et al., 1997). The data have first been decompressed and then flat-field corrected. The geometrical distortion of the detector was also corrected, using the standard destretching procedure of the SUMER software. The spectral pixels were then transformed into wavelengths by means of the calibration routines, and finally the measured intensity (in counts) of the lines was converted into radiometrically-calibrated spectral radiances (Wilhelm et al., 1997b, 1998a). The instrumental line broadening was also corrected for in the calculation of the Doppler line widths. Concerning the relative height in the solar atmosphere, we used the location of the maximum intensity in the radiance profile of the O I 924.952 Å line as a reference, which corresponds to the chromospheric plateau at a height of about 2 000 km, i.e. to about 3'' above the visible limb of the photosphere.

Fig. 1 shows the line profiles of L5, Ly6, Ly7, Ly9, Ly10 and Ly11 obtained at the relative heights between 15'' and 17'' above the maximum in the radiance profile of O I 924.952 Å. The crosses represent the observational data and the solid lines represent the Gaussian fits to the measurements. The fit is obtained by using the Gaussian-fit routine provided by IDL (Intercative Data Language). This fit includes a small linear and quadratic component to describe the slightly varying background. The quality of

Table 2. Effective Doppler speed

Height range	V_{eff} (km s ⁻¹)						Average
	Ly 5	Ly 6	Ly 7	Ly 9	Ly 10	Ly 11	
12'' – 15''				54		51	52.5 ± 1.5
15'' – 17''	66	57	56	51	51	47	54.7 ± 6
17'' – 19''	61	54	57			48	55.0 ± 5
19'' – 21''	62		61				61.5 ± 0.5
21'' – 23''	64						64

the fit may be evaluated by employing an index (named Gauss-fit error) that was suggested by Tu et al. (1998). For the Gauss fits shown in Fig. 1 the relative “errors” for Ly5 to Ly11 are 0.006, 0.018, 0.033, 0.014, 0.012, 0.009, respectively. Therefore, all fits are rather good.

Since the six Lyman lines considered here originate from the same hydrogen atom, we would expect the same kinetic temperature and turbulent broadening, and thus that the effective line widths should all be the same. However, we found that the line width decreased systematically from Ly5 to Ly11. This phenomenon is clearly apparent in Table 2, in which we show the effective Doppler speeds, which were calculated as $V_{eff} = 0.6006 \text{ FWHM } c/\lambda$ and correspond to the Gaussian-type line profile we obtained from this data set after subtraction of the instrument-related broadening. Here c is as usual the speed of light, λ the wavelength, and the abbreviation FWHM stands for the full width at half maximum of the line profile. We can see the general trend in the line width, which is that (with one exception: Ly6 obtained at 17''–19'') the lines become slightly narrower with increasing series or quantum number. This phenomenon has not yet been understood. It may be due to an increase of opacity with decreasing Lyman-line series number. Yet, why then do we still obtain excellent Gaussian line profiles at finite opacities? In this context it should be mentioned that Rosenberg et al. (1976) using Skylab data observed up to 26 members of the H I Balmer series at 2'' and 4'' above the limb in a polar coronal hole and found that the line widths (for $n \leq 15$) also decreased with increasing series number, n , which was interpreted as being due to opacity effects. If opacity really is broadening also the Lyman lines considered here, then this effect should perhaps decrease with height. Also, low opacity may produce line profiles that mimic Gaussians. In any case, detailed radiative transfer modelling as in Heinzel (1995) and Heinzel et al. (1997) is required to understand what is going on.

By inspection of the columns in Table 2, referring to the lines Ly7 and Ly5, one finds a trend of increasing V_{eff} with height, which is clearly visible with the exception of the top entry in the Ly5 column. Since the total data set is limited, as far as

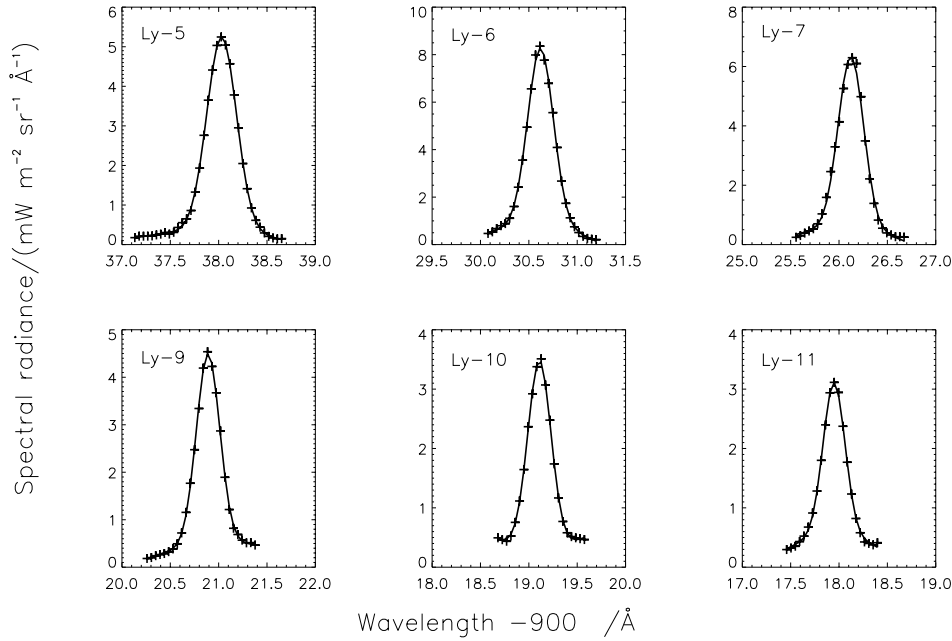


Fig. 1. Line profiles of six Lyman lines as observed by SUMER on 7 March 1999 in the north polar region of the Sun at height between $15''$ and $17''$ above the location of the maximum in the O I 924.952 Å radiance profiles. The crosses are the observational data, and the solid lines represent the corresponding Gaussian fits to the data. Note that the line width decreases with increasing series number.

the coverage of the line series is concerned, we averaged over these data at a given height bin. The average results are shown in the right column of Table 2. When assuming a reasonable turbulence amplitude of $\xi = 30 \text{ km s}^{-1}$ (consistent with earlier estimates by Brekke et al. (1997), Seely et al. (1997), Tu et al. (1998, 1999), Wilhelm et al. (1998b) and Marsch et al., (1999); see also the discussion below), we can calculate the variation of the kinetic temperature T_H with altitude by using the standard equation

$$V_{eff}^2 = \frac{2k_B T_H}{m_H} + \xi^2 \quad (1)$$

to convert the Doppler width into temperature. Here T_H is the temperature of the hydrogen atoms (and protons assuming charge-exchange equilibrium) along the line of sight, m_H is their mass, and ξ the turbulent speed.

The result of this averaging of our data is shown by the solid line in Fig. 2, which gives the mean hydrogen temperature versus height. The height, h , in the atmosphere is calculated simply from the number of spatial pixels, n_{px} , according to the simple formula: $h = (715 n_{px} + 2000) \text{ km}$. The dashed line is obtained from the data set 2, which is shown in addition to the actual data set 1 and reiterated for comparison with the previous paper by Marsch et al. (1999). Their data were also obtained in the northern polar hole of the Sun, albeit earlier in the phase of the solar cycle closer to minimum. We see that the temperatures derived from two data sets show a similar gradient, although slightly displaced. From $1.2 \cdot 10^4 \text{ km}$ to $1.8 \cdot 10^4 \text{ km}$, the temperature increases from $1 \cdot 10^5 \text{ K}$ to about $2 \cdot 10^5 \text{ K}$. From a log-log linear fit to these data, we find a temperature height profile: $T_H = 0.19 (h/\text{km})^{1.4} \text{ K}$. This temperature profile is comparatively flat when compared with the conventional empirical and physical TR models as reviewed by Mariska (1992). If extrapolated into the open corona, however, this profile would yield the canonical $1 \cdot 10^6 \text{ K}$ temperature slightly above the photosphere

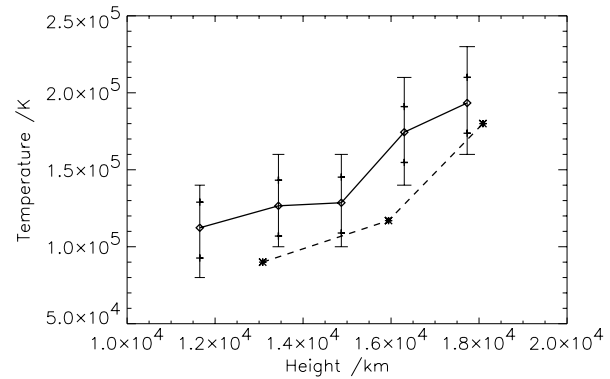


Fig. 2. Hydrogen temperature variation with height in the lower solar atmosphere. The diamonds (connected by a solid line) represent results from data set 1, and the asterisks (connected by a dashed line) results from data set 2. Both are calculated assuming $\xi = 30 \text{ km s}^{-1}$. The upper crosses are calculated assuming only $\xi = 25 \text{ km s}^{-1}$, while the lower crosses are for $\xi = 35 \text{ km s}^{-1}$, in order to give a feeling for the influence the value of ξ has on the temperature estimate. The error bars are calculated by assuming an uncertainty of 0.2 pixels in the evaluation of the line widths.

at about $1.1 R_\odot$ (here R_\odot means the solar radius) and much higher values beyond. Yet, the gradient is too steep in order to be consistent with the UVCS hydrogen measurements (Kohl et al., 1997, 1998) or the funnel-model results (Hackenberg et al., 2000), which yield about $2 \cdot 10^6 \text{ K}$ near $2 R_\odot$.

The reason why we chose $\xi = 30 \text{ km s}^{-1}$ is as follows. The effective Doppler speed of the simultaneously observed Fe III 929.163 Å line is found to be 28 km s^{-1} at $8''$ and 26 km s^{-1} at $6''$ in data set 1. Since the iron mass m_{Fe} is large as compared with m_H , we can conclude that the thermal speed of iron is much smaller than that of hydrogen at the same kinetic temperature, and that $V_{Fe,eff}$ is about equal to ξ and thus a good

proxy for the turbulence amplitude. This method to estimate ξ has successfully been used by Tu et al. (1998). Considering the WKB variation for the turbulence amplitude, this would imply the scaling with proton density, n_p , according to: $\xi \propto n_p^{-1/4}$. If the temperature increase by a factor of 2, the density should decrease by a factor of 2 to keep the pressure balanced locally. Correspondingly, ξ may increase by about 20 percent. We have also made calculations for $\xi = 25 \text{ km s}^{-1}$ and 35 km s^{-1} ; the results are marked in Fig. 2 by the upper and lower crosses, respectively. All these deviations are within the error bars as determined by an assumed uncertainty of 0.2 spectral pixels of the line-width estimates. Therefore, we assumed constant turbulence amplitudes in deriving the respective temperature gradients which are shown in Fig. 2.

3. Discussion

We used the technique described in Marsch et al. (1999) to analyse a SUMER data set of six emission lines of the H I Lyman series obtained in a northern polar coronal hole with long exposure time. These observations were done to corroborate our earlier findings and to establish values of the hydrogen (proton) temperature low in the solar atmosphere, to be used as reference points for solar wind models (see, e.g., the recent review by Marsch, 1999). We were able to derive the hydrogen temperature height profile in the TR and found new phenomena which we presently do not fully understand, namely an increase of the line width with decreasing Lyman series number and an unexpectedly flat hydrogen-temperature gradient.

A principal problem of any remote and off-limb observations of the solar TR and corona is that we cannot discriminate between individual plasma fine structures through which we may look along the line of sight (LOS), and which add to the accumulated line intensity as measured by the spectrometer. Even when looking off the limb above the nominal height of the solar TR region, if defined, e.g., by the top of the spicules in H_α , one cannot be sure that one does not sample merely radiation coming from thin elongated but magnetically confined strands of plasma (meso- or macro-spicules, see, e.g., Koutchmy & Loucif, 1991), which overshadow the radiation coming from the more dilute plasma which is flowing on open fields and contributes to the corona and solar wind. This could explain the flat temperature gradient. We cannot be sure that in our study we really saw the radiation coming from the boundaries of the coronal holes (open fields) proper, but that we looked perhaps more at dim ray-like features (laying in lateral scale between plumes and spicules), which do usually not show up in short-exposure images of the limb region below coronal holes.

The widening of the line widths with decreasing series number as shown in Fig. 1 may partly be caused by different absorptions along the LOS for the different lines, i.e. through different line opacities. However, that the shapes are well fitted by Gaussians seems to speak against this possibility, and suggests that these lines did not experience considerable intensity variation by absorption and re-emission, although low opacities may produce line profiles mimicking Gaussians. It is also possible that

some unknown process compensates for and masks the existing influence of line opacity.

The temperature profiles in Fig. 2 show that the hydrogen temperature increases by about 100 000 K in a 6 000 km height range. This temperature gradient is rather small in comparison with the predictions of the temperature profiles obtained in the classical TR (Mariska, 1992) models of an onion-shell-shaped solar atmosphere, or in models of coronal funnels (Gabriel, 1976; Marsch & Tu 1997; Axford & McKenzie, 1997; Hackenberg et al., 1999; Hackenberg et al., 2000), in which the heat conduction by electrons and protons plays a major rôle and produces very abrupt and steep temperature increases. If we can assume that we saw indeed plasma stemming from funnel flows in our data, then we would have to conclude that, unlike heat conduction in the models, probably some other unknown process controls the temperature in the height range between 12 000 km and 18 000 km, for example a small-scale (100 km or so) heating process that occurs intermittently over a wide range of heights.

It is also possible that our observations represent emissions from plasma sitting in different structures, in which the sharp “theoretical temperature jump” is located at different heights, so that the mixing of various jumps leads to a washed-out transition along the LOS. Then the disagreement with the classical TR models would not be surprising because, although every coronal loop probably has a sharp TR, most of the observed emission arises in cool loop-type structures. Since the classical TR is so thin the emission from the thin zones would be outshined by emission from the extended structures. The results we found may also represent the mixing of plasmas with varying opacity (and thus mixing optically thick and thin regions along the LOS), in which case there would be no fair chance of disentangling the observations and coming to reliable conclusions. Certainly, we have obtained a valuable reference temperature at the bottom of the corona (if seen on the scale of a solar radius) for large-scale solar wind models. Yet, to reach definite conclusions about the hydrogen (proton) temperature gradient between 2 000 km and 20 000 km demands observations at even higher resolution in space and time than is possible with SOHO, and also better knowledge of the magnetic field structure and geometry, which presently is in the TR only available from potential or force-free field model extrapolations of the photospheric field measurements.

Acknowledgements. The SUMER project is financially supported by DLR, CNES, NASA and the ESA PRODEX programme (Swiss contribution). We thank the SUMER operation team and the staff at the Experiment Operations Facility (EOF) of SOHO at GSFC in Greenbelt, USA, for their support in obtaining the observations. Parts of C.-Y. Tu’s work were supported by the National Natural Science Foundation of China under projects with contract numbers 49874036 and 49990452.

References

- Axford W.I., McKenzie J.M., 1997, in: Matthews M.S., Ruskin A.S., Guerrieri M.L. (eds.), *Cosmic Winds and the Heliosphere*, Tucson AZ: The University of Arizona Press, p. 31

- Brekke P., Hassler D.M., Wilhelm K., 1997, *Solar Phys.* 175, 349
- Chae J., Yun H.S., Poland A.I., 1998, *ApJS* 114, 151
- Curdt W., Kucera A., Rybak J. et al., 1997, Fifth SOHO Workshop, Oslo, Norway, ESA SP-404, 307
- Curdt W., Heinzel P., 1998, *ApJ* 503, L95
- Feldman U., Doscheck G.A., VanHoosier M.E. et al., 1976, *ApJS*, 31, 445
- Fludra A., Brekke P., Harrison R.A. et al., 1997, *Solar Phys.* 175, 487
- Gabriel A.H., 1976, *Phil. Trans. R. Soc. London* 281, 339
- Hackenberg P., Mann G., Marsch E., 1999, *Space Sci. Rev.*, 87, 201
- Hackenberg P., Marsch E., Mann G., A&A, 2000, submitted
- Heinzel P., 1995, A&A 299, 563
- Heinzel, P., Schmieder, B., Vial, J.-C., 1997, Fifth SOHO Workshop, Oslo, Norway, ESA SP-404, 427
- Kohl J.L., Noci G., Antonucci E., et al., 1997 *Solar Phys.* 175, 613
- Kohl J.L., Noci G., Antonucci E., et al., 1998 *ApJ Letters* 501, L127
- Koutchmy S., Loucif M.L., 1991, in: Ulmschneider P., Priest E.R., Rosner R. (eds.), *Mechanisms of Chromospheric and Coronal Heating*, Heidelberg: Springer-Verlag, p. 152
- Lemaire P., Wilhelm K., Curdt W. et al., 1997, *Solar Phys.* 170, 105
- Mariska J.T., 1992, *The Solar Transition Region*, Cambridge: Cambridge University Press
- Marsch E., 1999, *Space Science Rev.*, 87, 1
- Marsch E., Tu C.-Y., 1997, *Solar Phys.* 176, 87
- Marsch E., Tu C.-Y., Wilhelm K. et al., 1997, ESA SP-404, 555
- Marsch E., Tu C.-Y., Heinzel, P. et al., 1999, A&A 347, 676
- Rosenberg F.D., Feldman U., Doscheck G.A., 1976, *ApJ* 212, 905
- Seely J.F., Feldman U., Schühle U. et al. 1997, *ApJ* 484, L87
- Tu C.Y., Marsch E., Wilhelm K. et al., 1998, *ApJ* 503, 475
- Tu C.Y., Marsch E., Wilhelm K., 1999, *Space Sci. Rev.* 87, 331
- Warren H.P., Mariska J.T., Wilhelm K., 1998 *ApJS* 119, 105
- Wilhelm K., Curdt W., Marsch E. et al., 1995, *Solar Phys.* 162, 189
- Wilhelm K., Lemaire P., Curdt W. et al., 1997a, *Solar Phys.* 170, 75
- Wilhelm K., Lemaire P., Feldman U. et al., 1997b, *Appl. Opt.* 36, 6416
- Wilhelm K., Lemaire P., Dammasch I.E. et al. 1998a, A&A 334, 685
- Wilhelm K., Marsch E., Dwivedi B.N. et al. 1998b, *ApJ* 500, 1023
- Vernazza J.E., Avrett E.H., Loeser R., 1973, *ApJ* 184, 605
- Vernazza J.E., Avrett E.H., Loeser R., 1981, *ApJ Suppl.* 45, 635